A Maximum Entropy Algorithm for Holographic Structure Completion in Macromolecular X-ray Crystallography

D. K. Saldin and V. L. Shneerson

Department of Physics and Laboratory for Surface Studies, University of Wisconsin-Milwaukee, P.O. Box 413, Milwaukee, Wisconsin 53201, U. S. A.

and D. L. Wild

Structural Biology Laboratory, The Salk Institute, 10010 N. Torrey Pines Road, La Jolla, California 92037, U. S. A.

We discuss the historical origin of the holographic concept in the field of crystallography and its relation to modern applications of similar ideas to the problem of structure completion in macromolecular x-ray crystallography. For structure completion, the identification of the diffracted amplitude from the known part of the structure with a reference wave enables the recovery of the unknown part of the electron density from the diffraction intensities. In this article, we show how this may be achieved by means of a maximum entropy algorithm.

Journal of Imaging Science and Technology 41: 482–487 (1997)

Introduction

Holography is a subject that today is most familiar in its optical applications and, particularly, in its apparent ability to store and reconstruct three-dimensional images that appear suspended in thin air. In fact, the main expansion of the field of optical holography[1] did not occur until the 1960s, following the development of the laser with its ability to generate light with coherence lengths of the order of about a meter. A study of the historical record shows that holography owes its invention more to the subject of crystallography than optics.

In this article we discuss the relation between the historical origins of the holographic concept and its modern application to the problem of structure completion in the x-ray crystallography of proteins.[2–4] For structure completion, the idea exploited is that during structure solution a partial model of the molecule may have been constructed with the remainder unknown. Treating the diffraction amplitudes from the known parts of the structure as a reference wave, an algorithm based on the conjugate gradient method was used[4] to determine the electron density from the unknown part using the information from the diffraction pattern now interpreted as a hologram.

We propose and demonstrate the effectiveness of an alternative algorithm, based on the maximum entropy principle,[5] for implementing a holographic scheme for the problem of structure completion in the x-ray crystallography of biological macromolecules.

Original manuscript received January 18th, 1997.

Crystallography—The Original Inspiration for Holography

In his famous article that marked the invention of holography, Gabor[6] acknowledged his debt to prior ideas from the field of x-ray crystallography. The basic task in that field is to recover the spatial distribution of the electron density within the unit cell of a crystal from measured intensities of Bragg spots on a diffraction pattern.

If the amplitude of a Bragg reflection is written

$$A_g = \sum_j f_j \exp\{i\mathbf{g}\cdot\mathbf{r}_j\}, \tag{1}$$

where f_j is the scattering factor of the atom j at a position $\mathbf{r}_j$ within a unit cell, the corresponding intensity on a diffraction pattern is

$$I_g = \sum_{j,k} f_j^* f_k \exp\{i\mathbf{g}\cdot(\mathbf{r}_k - \mathbf{r}_j)\}. \tag{2}$$

The stationary-phase condition shows that any attempt to recover the structure of the unit cell by a direct Fourier transformation of the measured data by an algorithm of the form

$$U(\mathbf{r}) = \int I_g \exp\{-i\mathbf{g}\cdot\mathbf{r}\} \tag{3}$$

will yield a function $|U(\mathbf{r})|^2$ that peaks at positions $\mathbf{r}$ equal to $\mathbf{r}_k - \mathbf{r}_j$ for all values of k and j. In other words, such a simple Fourier transform can yield only the pair-correlation function, or Patterson function as it is known in x-ray crystallography. In general, such a function is insufficient to determine a structure fully.

An important early insight was the realization that if one of the atoms in the unit cell had a scattering factor f_0,

for example, that was much larger than the others, much more information could be obtained about the structure by a transform of the same form as Eq. 3. Placing the heavy atom at the origin of the coordinate system, Eq. 2 may be written as

$$I_g = |f_0|^2 + f_0^* \sum_{j\neq 0} f_j \exp\{i\mathbf{g}\cdot\mathbf{r}_j\} + f_0 \sum_{j\neq 0} f_j^* \exp\{-i\mathbf{g}\cdot\mathbf{r}_j\} + \sum_{j\neq 0}\sum_{k\neq 0} f_j^* f_k \exp\{i\mathbf{g}\cdot(\mathbf{r}_k - \mathbf{r}_j)\}. \quad (4)$$

It is apparent that if

$$|f_0| >> |f_j| \quad (5)$$

for all $j \neq 0$, then the double summation in Eq. 4 may be neglected. Consequently, application of a transform of the form of Eq. 3 to the remaining terms in Eq. 4 will yield a function $|U(\mathbf{r})|^2$ that would be expected to peak at positions $\mathbf{r} = 0$, $\mathbf{r}_j$, and $-\mathbf{r}_j$. If, in addition, the heavy atom is at the center of a centro-symmetric unit cell, even the value $-\mathbf{r}_j$ will mark an atom location, and thus the function $|U(\mathbf{r})|^2$ will correctly map the relative atom positions within the unit cell.

Early in the development of x-ray crystallography, Bragg[7,8] invented an ingenious device that he called an x-ray microscope, that exploited the above idea to recover directly the projection, along one of the crystal axes, of the electron density of a unit cell of a substance with 2-D projection of the above type.

The point of the heavy-atom method is that if the amplitude from one of the atoms is very large, the diffraction pattern consists basically of the sum of the intensity from that atom and the interference between the amplitudes from the known heavy atom and those from the unknown scatterers. This is the feature used in all holographic methods.

Structure Completion in x-ray Crystallography

Formulation of the Problem. Now let us move the clock forward to the modern era in x-ray crystallography where researchers are grappling with ever more complicated structures, such as those of biological macromolecules. In the process of determining the structures of macromolecules, modern crystallographers may be faced with the need to reconstruct a missing part of the molecule from the knowledge of a partial model and the measured diffraction intensities.

This problem is reminiscent of the heavy-atom method, except now the known part of the structure plays the role of the heavy atom. But, unlike the case considered earlier, we require a technique that would work for any type of crystal symmetry. The holographic method proposed recently by Szöke and colleagues[2–4] regards the contributions to the Bragg amplitudes from the known part of the structure as a reference wave and those from the unknown part as an object wave. The x-ray diffraction pattern is regarded as a hologram, and one seeks an algorithm that can recover the object wave and, hence, the missing part of the structure in analogy with the holographic reconstruction process.

Suppose that the unit cell of the crystal is divided into a set of voxels centered on a uniform grid of points. Let the number of electrons from the known part of the structure in the voxel centered on the position $\mathbf{r}_i$ be n_i. Then the contribution from the known part of the structure to the amplitude of the Bragg reflection $\mathbf{g}$ will be given by the discrete Fourier transform:

$$R_g = \sum_i n_i \exp(i\mathbf{g}\cdot\mathbf{r}_i). \quad (6)$$

The set of amplitudes $R_\mathbf{g}$ may be identified with a holographic reference wave. If the set of contributions to the same Bragg amplitudes from the unknown part of the electron density in the unit cell are represented by $O_\mathbf{g}$, the total intensity of the Bragg reflection may be written

$$I_\mathbf{g} = |A_\mathbf{g}|^2, \quad (7)$$

where

$$A_\mathbf{g} = R_\mathbf{g} + O_\mathbf{g}. \quad (8)$$

The recovery of the unknown amplitudes $O_\mathbf{g}$ from a set of measured intensities $I_\mathbf{g}$ and the known amplitudes $R_\mathbf{g}$, is the classic problem of holography. Of course, once the complete set of object wave amplitudes, $O_\mathbf{g}$ is recovered, the electron distribution $\{u_i\}$, defined on the same voxel grid, may be found by an inverse Fourier transform.

As a test case, we considered the molecule of the protein bovine pancreatic trypsin inhibitor (BPTI), also considered by Maalouf *et al.*[3] We took the atomic coordinates listed for BPTI in the Protein Data Bank (entry 6PTI) and used them to calculate the structure factors $A_\mathbf{g}$ to 3-Å resolution, using standard crystallographic software. A known partial structure was produced by deleting the atoms comprising amino acid residues 1 through 28 (approximately 50% of the structure) and the remaining atomic coordinates used to calculate $R_\mathbf{g}$.

The best estimate of the electron distribution in the deleted amino acid residues that may be reconstructed from data of such resolution is then given by

$$u_i = \frac{1}{N}\sum_\mathbf{g}\{A_\mathbf{g} - R_\mathbf{g}\}\exp(-i\mathbf{g}\cdot\mathbf{r}_i), \quad (9)$$

where N is the number of Bragg reflections $\mathbf{g}$ in the sum above, and we make use of the fact that in our model problem the complete amplitudes (moduli and phases) of both $A_\mathbf{g}$ and $R_\mathbf{g}$ are known.

The structure factors used in all the work reported in this article corresponded to maximum Miller indices of $h_{max} = 18$, $k_{max} = 12$, and $l_{max} = 8$ in the positive octant of reciprocal space. These were extended to all eight octants by applying the appropriate symmetry relations. Because all Fourier transforms in the present work were performed with the fast Fourier transform algorithm FOURN of Press et al.,[9] that requires array dimensions of powers of 2, we expanded our reciprocal space arrays to dimensions of $64 \times 32 \times 32$ covering all eight octants by assigning zero structure factors to all of the reciprocal lattice points with unassigned values. Consequently, the number of real-space grid points in the unit cell of dimensions $a = 55.20$, $b = 38.20$, and $c = 24.05$ Å was also $64 \times 32 \times 32$, corresponding to grid spacings of 0.86, 1.19, and 0.75 Å in the directions of the respective unit vectors.

The result of using Eq. 9 to calculate the electron distribution in the deleted amino acid residues 7 through 22 is shown in Fig. 1. The stereo pair of diagrams, produced by the SETOR program[10] shows an isosurface corresponding to an electron density of 1.5 times the rms deviation above the mean. This surface is indicated by a

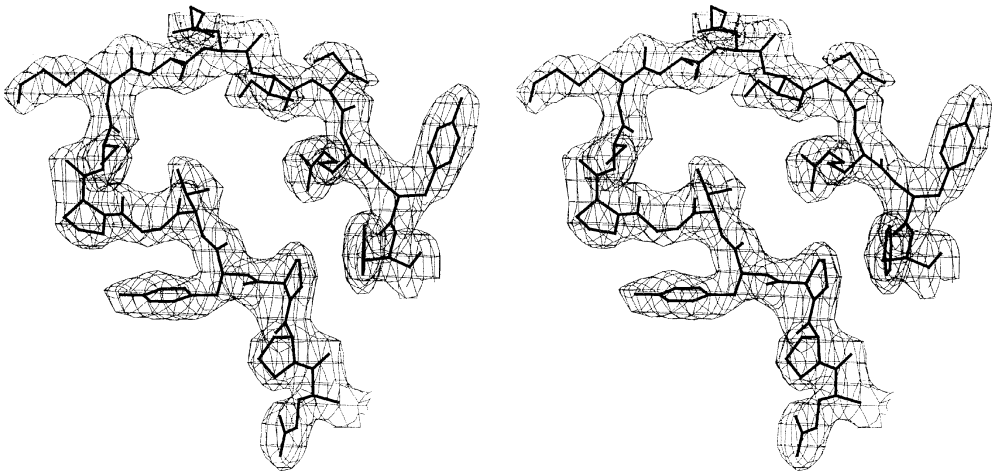

Figure 1. A stereo pair showing the surface of the known 3-D electron density of residues 7 through 22 of bovine pancreatic trypsin inhibitor (BPTI) corresponding to a density of 1.5 times the rms variation of the map above the mean density. The fit to the stick figure representing the bonds of the residues 7 through 22 is excellent. Note that the 3-D nature of the reconstructed electron density and the stick figure are best revealed with the use of a stereo viewer.

wire mesh representation. A comparison with the stick figure of the bonds of the deleted amino acids shows a very close fit as is to be expected. This will represent the ideal electron density of the unknown part of the structure that we will reconstruct by the two practical methods described next.

Difference Fourier Method. An approximate method for determining the unknown electron distribution $\{u_i\}$ from data actually available in a typical problem in x-ray crystallography and that works well if the missing part is a relatively small part of the entire electron distribution in the unit cell is called the difference Fourier method.[11] Of course, such a method cannot assume any knowledge of the phases of the Bragg reflections $\mathbf{g}$, and it approximates u_i at the point $\mathbf{r}_i$ by

$$u_i = \frac{1}{N}\sum_{\mathbf{g}}\left\{\left|A_{\mathbf{g}}\right|\exp\left(i\phi_{\mathbf{g}}^{(R)}\right) - R_{\mathbf{g}}\right\}\exp\left(-i\mathbf{g}\cdot\mathbf{r}_i\right), \quad (10)$$

where

$$\phi_{\mathbf{g}}^{(R)} = \arg(R_{\mathbf{g}}) \quad (11)$$

is the phase of $R_{\mathbf{g}}$, which is known because it is derived from a calculation of $R_{\mathbf{g}}$ from the known part of the structure.

For the same test case as that noted previously, Eq. 10 was used to recover the three-dimensional electron distribution of the deleted amino acid residues 1 through 28. The reconstructed electron density of residues 7 through 22 is shown in Fig. 2, also as a stereo pair. In this case the wire mesh surface depicted has been contoured at a value of 0.5 times the rms deviation above the mean electron density. Comparison with the stick figure of the bonds of the same deleted amino acids shows some incorrect connectivity and other regions of false electron density.

As a measure of the effectiveness of the difference Fourier method in recovering the distribution of electrons in the missing amino acids, we computed the linear correlation coefficient[9] between the recovered distribution and the exact one calculated from Eq. 9. The value of this correlation coefficient for the difference Fourier distribution above was 0.53, signifying only moderate correlation.

Maximum Entropy Method. A more accurate holographic reconstruction algorithm for recovering $\{u_i\}$ has been developed by Szöke and co-workers.[2–4] That algorithm performs a minimization of a cost function with the aid of a conjugate gradient algorithm. As such, it depends on the result of the first iteration lying within the basin of the global minimum of the cost function. We have developed an alternative holographic reconstruction algorithm based on the maximum entropy method.[5]

The basic idea of the maximum entropy method is to make the least unbiased guess of a distribution, subject to constraints imposed by any firm knowledge about the distribution. In our problem what is sought is the electron distribution in an unknown part of a structure and constraints are imposed by the known intensities of measured Bragg reflections. In mathematical terms, we seek an electron distribution

$$\left\{u_i^{(n)}\right\}$$

at the nth iteration of our algorithm from the estimate

$$\left\{u_i^{(n-1)}\right\}$$

from the previous iteration by finding that which maximizes the functional

$$Q\left[\left\{u_i^{(n)}\right\}\right] = -\sum_i u_i^{(n)} \ln\left[\frac{u_i^{(n)}}{e u_i^{(n-1)}}\right] - \frac{\lambda'}{2}\sum_{\mathbf{g}}\frac{\left|O_{\mathbf{g}}^{(n)} - T_{\mathbf{g}}^{(n)}\right|^2}{\sigma_{\mathbf{g}}^2}, \quad (12)$$

where the first term on the right side is an expression for the entropy of the distribution

$$\left\{u_i^{(n)}\right\}$$

with respect to a prior one

$$\left\{u_i^{(n-1)}\right\}$$

from a previous iteration. The second term on the right side constrains the calculated Bragg amplitudes

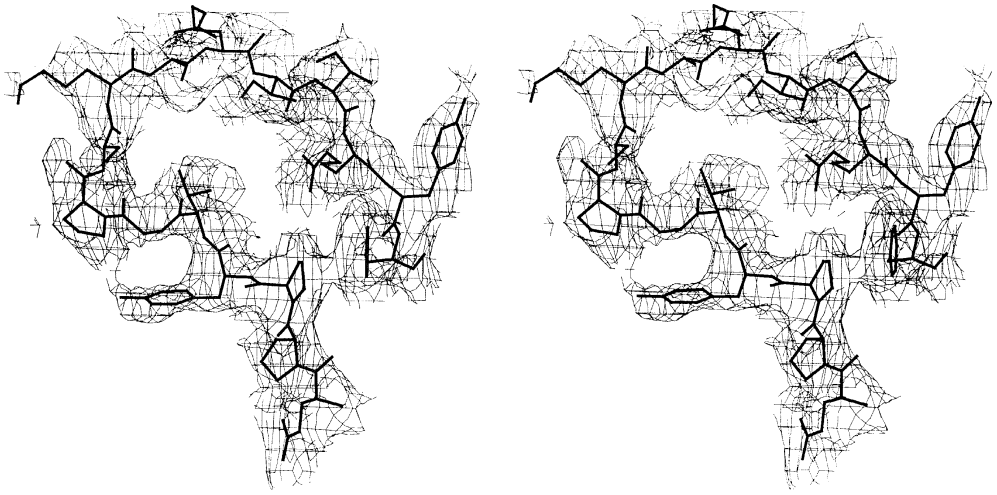

Figure 2. Same as Fig. 1 except that the electron density shown is that recovered by the standard unweighted difference Fourier method from the model Bragg reflection intensities of the entire molecule and a knowledge of the electron density of the molecule with residues 1 through 28 (i.e., 50% of molecule) deleted. The surface indicated by the wire mesh is that corresponding to an electron density of 0.5 times the rms deviation of the density above the mean. Some false connectivity and other incorrect electron density reconstructions are apparent.

$$O_{\mathbf{g}}^{(n)} = \sum_i u_i^{(n)} \exp(i\mathbf{g}\cdot r_i) \tag{13}$$

from the unknown part of the structure to be consistent with the experimental data, represented by a set of target amplitudes

$$T_{\mathbf{g}}^{(n)} = \left\{ \left| A_{\mathbf{g}} \right| \exp\left(i\phi_{\mathbf{g}}^{(n)} \right) - R_{\mathbf{g}} \right\}, \tag{14}$$

where $\sigma_{\mathbf{g}}$ represents the standard deviation in the measurement of $|A_{\mathbf{g}}|$,

$$\phi_{\mathbf{g}}^{(n)} = \arg\left(R_{\mathbf{g}} + O_{\mathbf{g}}^{(n)} \right) \quad \text{if } n \geq 2, \tag{15}$$

and λ' is a Lagrange multiplier.

The value Q may be maximized by requiring that

$$\frac{\partial Q}{\partial u_i^{(n)}} = 0 \text{ for all } i. \tag{16}$$

If we consider all the standard deviations $\sigma_{\mathbf{g}}$ constant, as we may do in the case of the synthetic data we consider here, we obtain the "single voxel" equations

$$\ln\left[\frac{u_i^{(n)}}{u_i^{(n-1)}} \right] = -\lambda \left\{ u_i^{(n)} - \tau_i^{(n)} \right\}, \tag{17}$$

where $\lambda = \lambda' N / \sigma_{\mathbf{g}}^2$ and

$$\tau_i^{(n)} = \frac{1}{N} \sum_{\mathbf{g}} T_{\mathbf{g}}^{(n)} \exp(-i\mathbf{g}\cdot r_i) \tag{18}$$

is a *target function* consisting of the inverse Fourier transform of $T_{\mathbf{g}}^{(n)}$. Approximating terms on the right side of Eq. 17 by their values at the previous iteration suggests the following algorithm for successively improving the estimate of u_i:

$$u_i^{(n)} = u_i^{(n-1)} \exp\left[-\lambda \left\{ u_i^{(n-1)} - \tau_i^{(n-1)} \right\} \right]. \tag{19}$$

We began our test calculation at the first iteration (n = 1) by assuming a form for $u_i^{(0)}$ based on a partial solvent mask calculated from a low-pass filtered electron distribution obtained by multiplying the structure factors ($A_{\mathbf{g}} - R_{\mathbf{g}}$) by a Gaussian envelope corresponding to 10-Å resolution. In addition, at the first iteration, $\tau_i^{(0)}$ was evaluated from Eq. 18 by taking

$$\phi_{\mathbf{g}}^{(0)} = \phi_{\mathbf{g}}^{(R)}, \tag{20}$$

as the phase of $R_{\mathbf{g}}$.

The iterations may be halted when convergence is reached [i.e., when $u_i^{(n)} \simeq u_i^{(n-1)}$ for all i]. As this limit is approached, Eq. 19 may be approximated by

$$u_i^{(n)} - u_i^{(n-1)} = \lambda u_i^{(n-1)} \left\{ \tau_i^{(n-1)} - u_i^{(n-1)} \right\}. \tag{21}$$

This equation shows that u_i converges toward (a simultaneously updated) target value τ_i provided

$$\lambda u_i^{(n-1)} \leq 1. \tag{22}$$

Because λ has the same value for all voxels, Collins[13] suggested taking

$$\lambda = 1/u_{\max} \tag{23}$$

where $u_{\max}$ is the maximum value of the distribution $\left\{ u_i^{(n-1)} \right\}$.

In our present case, this would correspond to a value of λ of the order of unity. For his problem of improving the resolution of a pre-existing map of an entire protein, Collins[13] reported results from just four iterations. However, note that condition 22 does not put a lower bound on λ. It may be seen from Eq. 12 that the lower the value of λ,

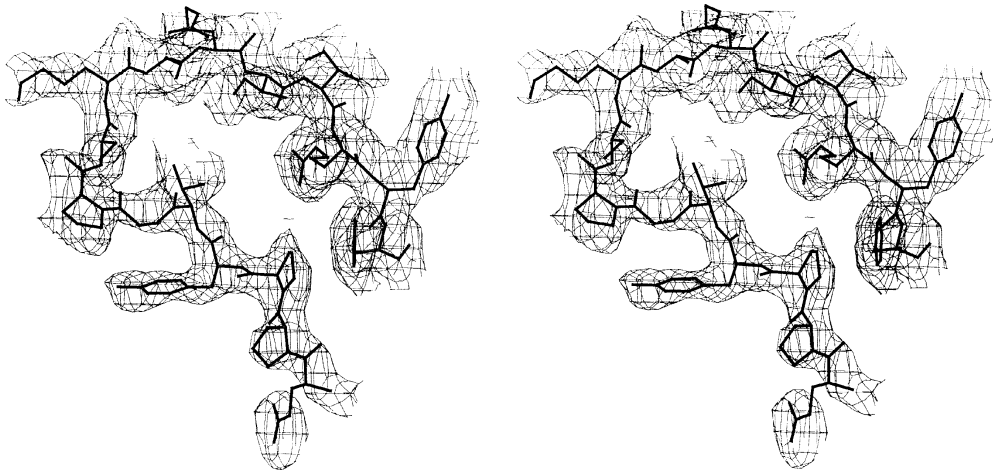

Figure 3. Same as Fig. 2 except that the electron density of residues 1 through 28 was reconstructed by the holographic maximum entropy algorithm. The wire mesh surface corresponds to an electron density of 1.0 times the rms deviation of the density above the mean. This electron density distribution gives a clear indication of the 3-D configuration of the missing residues 7 through 22 and is, in general, much closer to the true electron density of Fig. 1 than the difference Fourier density of Fig. 2.

the greater the role the entropy plays in the approach to convergence. In our calculations on the structure completion problem, where our starting point may be further from the true solution, we found it necessary to use a substantially lower value of λ than that in Eq. 23 suggested by Collins. In the computations reported here, we chose $\lambda \sim 3 \times 10^{-3}$. This resulted in a significantly slower rate of convergence. Fortunately, the dramatic increases in accessible computer power in the 15 years since Collins' work enabled us to perform our calculations in a reasonable time on a modern computer workstation.

Comparing Eqs. 18 and 14 with 10 highlights the difference between this maximum entropy algorithm and that of the difference Fourier method. Although, like the difference Fourier method, maximum entropy approximates the phases $\phi_{\mathbf{g}}^{(0)}$ of the full structure factors $A_{\mathbf{g}}$, by those, $\phi_{\mathbf{g}}^{(R)}$, of the known part of the structure at its first iteration, the maximum entropy method allows the subsequent refinement of these phases via Eq. 15 using an updated best estimate of the unknown part of the electron distribution.

The electron distribution in the same deleted side chains 1 through 28 of BPTI was calculated by algorithm 19, taking a Lagrange multiplier λ, whose value was adjusted at each iteration to keep the magnitude of the argument of the exponential in Eq. 19 constant. The result after 13,000 iterations (which took a few hours on a Silicon Graphics Indigo^2 workstation) is shown in Fig. 3, in which the electron density isosurface is plotted corresponding to 1.0 times the rms deviation of the density above the mean. The 3-D configuration of the missing amino acid residues 7 through 22 are here seen recovered with much greater fidelity in comparison with that from the difference Fourier algorithm shown in Fig. 2, as may be judged by comparison with the stick figure of the amino acid chains.

When used to compare the electron distribution in the missing chains recovered by this maximum entropy algorithm to the corresponding ideal distribution from Eq. 9, the value of the linear correlation coefficient[9] was 0.74, representing a 40% improvement in fidelity from the difference Fourier result of the previous section, and, hence, good correlation with the ideal electron density. We found improvements for deletions of other parts of the molecule, and conclude, as did Somoza et al.,[4] that a holographic reconstruction algorithm is a distinct improvement over the difference Fourier method for the recovery of unknown parts of a structure given knowledge of as little as 50% of the molecule. The new feature reported here is that the reconstruction may be performed by a maximum entropy algorithm similar to that used by Collins[13] for improving the quality of an electron density map of an entire molecule.

A similar algorithm was also used recently by Moritz and colleagues[14] and by us[15] for the direct recovery of surface electron density from crystal truncation rods in surface x-ray diffraction. In future work we may also experiment with alternative maximum entropy algorithms suggested by Bricogne and co-workers,[16–19] as recently reviewed by Gilmore.[20]

Conclusions

For didactic purposes, we have drawn attention to the close parallels between the recently proposed holographic method[2–4] for macromolecular x-ray crystallography, and the work of Bragg[7,8] which according to Gabor[6] provided the original inspiration for holography.

In this article we proposed and demonstrated the effectiveness of a method of solving the problem of structure completion in macromolecular x-ray crystallography based on the maximum entropy principle. We compared the electron distribution of the unknown part of the structure as reconstructed by our proposed algorithm with that from the standard difference Fourier method and the ideal result. We find the electron density map reconstructed by our algorithm to be significantly closer to the correct density than that from the difference Fourier method. ▲

Acknowledgments. D. K. S. wishes to acknowledge stimulating discussions with Wolfgang Moritz and Herbert Vogler on maximum entropy formalism and support for this work from the U. S. National Science Foundation (Grant No. DMR-9320275).

Referenes

1. R. J. Collier, C. B. Burkhardt, and L. H. Lin, *Optical Holography*, Academic Press, San Diego, 1971.
2. A. Szöke, Holographic methods in x-ray crystallography. II. Detailed theory and connection to other methods of crystallography, *Acta Cryst. A* **49**, 853 (1993).

3. G. J. Maalouf, J. C. Hoch, A. S. Stern, H. Szöke, and A. Szöke, Holographic methods in x-ray crystallography. III. First numerical results, *Acta Cryst. A* **49,** 866 (1993).
4. J. R. Somoza, H. Szöke, D. M. Goodman, P. Béran, D. Truckses, S.-H. Kim, and A. Szöke, Holographic methods in x-ray crystallography. IV. A fast algorithm and its application to macromolecular crystallography, *Acta Cryst. A* **51,** 691 (1995).
5. E. T. Jaynes, Information theory and statistical mechanics, *Phys. Rev.* **106**, 620 (1957).
6. D. Gabor, A new microscopic principle, *Nature* **161**, 777 (1948).
7. W. L. Bragg, A new type of x-ray microscope, *Nature* **143**, 678 (1939).
8. W. L. Bragg, The x-ray microscope, *Nature* **149**, 470 (1942).
9. W. H. Press, S. A. Teukolsky, W. T. Vetterling, and B. P. Flannery, *Numerical Recipes in FORTRAN*, 2nd ed., Cambridge University Press, 1992, p. 630.
10. S. V. Evans, SETOR: Hardware lighted three-dimensional solid model representations of macromolecules, *J. Mol. Graphics* **11**, 134 (1993).
11. W. Cochran, Some properties of F_o - F_c synthesis, *Acta Cryst.* **4**, 408 (1951).
12. S. F. Gull and G. J. Daniell, Image reconstruction from incomplete and noisy data, *Nature* **272**, 686 (1978).
13. D. M. Collins, Electron density images from imperfect data by iterative entropy maximization, *Nature* **298**, 49 (1982).
14. W. Moritz, private communication.
15. V. L. Shneerson, D. K. Saldin, H. Vogler, and W. Moritz, Direct recovery of surface electron density from crystal truncation rods in surface x-ray diffraction, *Bull. Amer. Phys. Soc.* **42**, 274 (1997).
16. G. Bricogne, Maximum entropy and the foundations of direct methods, *Acta Cryst. A* **40,** 410 (1984).
17. G. Bricogne, A Bayesian statistical theory of the phase problem: I. A multichannel maximum-entropy formalism for constructing generalized joint probability distributions of structure factors, *Acta Cryst. A* **44**, 517 (1988).
18. G. Bricogne, The x-ray crystallographic phase problem, in *Maximum Entropy in Action*, Oxford University Press, Oxford, 1991, p. 187.
19. G. Bricogne, Direct phase determination by entropy maximization and likelihood ranking: status report and perspectives, *Acta Cryst. D* **49**, 37 (1993).
20. C. J. Gilmore, Maximum entropy and Bayesian methods in crystallography: A review of practical applications, *Acta Cryst. A* **52**, 561 (1996).